Integrating phase change materials into concrete through microencapsulation using cenospheres

Fengjuan Liu, Jialai Wang*, Xin Qian

Department of Civil, Construction and Environmental Engineering, The University of Alabama, Tuscaloosa, AL 35487, United States

ABSTRACT

Phase change materials (PCMs) can enhance the building energy efficiency through Thermal Energy Storage and thermal regulation. Microencapsulated PCMs (MEPCMs) provide a better utilization of PCMs with building materials. This study proposes a novel method to encapsulate PCMs into cenospheres which are hollow fly ash particles generated in coal burning power plants with size ranging from a few micrometers to hundreds of micrometers. The shell of the cenosphere inherently has some small pores which are sealed by a thin layer of glass-crystalline film. By removing this film through chemical etching, these holes can be exposed, providing paths for PCMs moving into the internal void of cenospheres. A thin layer of silica is coated on the PCM loaded cenospheres to prevent the possible leakage of liquid PCMs. The produced PCM microcapsules are referred to as CenoPCM, which can be directly added into traditional construction and building materials such as concrete to produce thermally active concrete. Prototype thermally active cement mortar integrated with the produced CenoPCM capsules have also been manufactured and characterized for its mechanical and microstructural properties. The characterizations showed that there was only minor reduction in strength and the mortar remained strong enough for building application. From this work, it is found that the produced

* Corresponding author. Tel.: +1-305-3486786; fax: +1-205-348-0783.
E-mail address: jwang@eng.ua.edu

CenoPCM capsules have great potential to be added into construction materials for reducing energy consumptions in buildings.

Keywords: Thermal energy storage, Phase change materials, Cenospheres, Microencapsulation, Concrete

1. Introduction

It is estimated by the World Business Council for Sustainable Development that buildings are responsible for at least 40% of energy use in many countries [1]. Energy use is increasing at an annual rate of more than 3% in the U.S. alone, and is growing rapidly in countries such as China and India. Worldwide energy consumption by buildings is expected to grow 45% over the next 20 years. To cope with this challenging situation, efforts are needed to improve the energy efficiency of buildings, which will not only relieve the energy demands, but also reduce the environmental impacts associated with energy use, e.g. carbon dioxide emission.

Integrating phase change materials (PCMs) into building materials has been proposed to address this need. PCMs can enhance the building energy efficiency through Thermal Energy Storage (TES) and thermal regulation [2]. PCMs change their phase from solid to liquid and vice versa at their phase change temperatures with large amounts of energy absorbed or released. Thermal inertia (mass) of the building can be significantly increased by the integration of PCMs. PCM-enhanced building envelopes have been studied with the following aspects in mind: narrowing the gap between the peak and off-peak loads, saving building operation costs under specific electricity tariffs, reducing diurnal temperature fluctuations concerning the occupants' thermal comfort, and utilizing the free cooling at night for day peak cooling load shaving, along

with others [3–6]. Significant energy savings for buildings can be achieved by PCMs, as demonstrated by extensive studies [7,8].

Directly employing bulk PCMs into building materials suffers a few drawbacks. For example, special latent heat devices or heat exchange surfaces are needed, which increases the associated cost and thermal resistance between the PCM and the environment. Therefore, two methods are commonly used to incorporate PCM into construction materials: microencapsulation of PCMs and form-stable PCM composites. In the first method, PCMs are encapsulated within a protection shell with a size between 1 and 300 μm [9]. The produced microencapsulated PCMs (MEPCMs) can preserve PCMs as long as the shell is intact during heating/cooling cycles. MEPCMs provide a better utilization of PCMs within building components such as walls, roofs, and floors, and within the building materials such as concrete, gypsum wallboard, plaster, and mortar, among others. Compared with traditional PCMs, MEPCMs enjoy many advantages such as their chemically-inert nature (due to the polymer barrier between the PCM and any other material), the optimized heat transfer due to a high surface-area-to-volume ratio, and their ability to be readily mixed into or coated onto other materials [8,10].

However, MEPCMs also suffers a few drawbacks preventing their extensive application in construction materials. First, the protection shell is usually made of polymer, which is of low mechanical stiffness and strength. As a result, the mechanical stiffness and strength of the construction materials can be significantly reduced by adding the PCMs microcapsules [11,12]. Because of the low mechanical properties, PCMs microcapsules can also be broken during the mixing of concrete, leading to the leakage of PCMs after melting. Second, the polymeric shell also has low chemical and thermal stability, which can be deteriorated by UV light, oxidation, and other aggressive chemicals. The shell can lose its stability when temperature exceeds its

glass transition temperature, and it is flammable, and therefore cannot be adopted by US building industry. Finally, the thermal conductivity of the polymer shells is very low, making thermal exchange between PCMs inside the shell and outside environment much more difficult [13,14].

In the second method, PCMs are first absorbed into porous materials such as light weight aggregates and diatomite particles to form stable composites, which are then added into the construction materials [15–18]. While in absorbing PCM using porous particles, no protective layers on the surface of the composites are available. As a result, PCMs can still leak from the porous material during its melting process, leading to the reduction or loss of the claimed thermal storage capacity.

To facilitate more extensive and practical application of PCM in construction materials, the above barriers must be removed. To this end, this study proposes a novel method to encapsulate PCMs with cenospheres, which are hollow fly ash particles generated in coal burning power plants. Cenosphere particles have an aluminosilicate shell with high stiffness, high strength, and a thickness of a few micrometers. The shell has a porous structure formed by gas inclusion and is covered by a layer of glass-crystalline nanosize film [19]. The hollow structure of the cenosphere makes it an ideal material to encapsulate PCM. However, to introduce PCM into a cenosphere, the glass-crystalline nanosize film on the surface of the cenosphere must be removed. This is done by acid etching in this study. After removing the thin film, perforated cenospheres with very small holes penetrating through the shell can be produced. By simply mixing the perforated cenospheres in liquid PCM, liquid PCM can be loaded into the perforated cenospheres via a vacuum impregnation process. A thin layer of silica coating is then applied to the PCM loaded perforated cenospheres to prevent the possible leakage of liquid PCMs. The produced PCM microcapsules with cenosphere shell are therefore referred to as CenoPCM in this study.

With cenospheres, the expensive process to synthesize the polymer shell used in existing MEPCMs is therefore eliminated. As a result, the cost to produce PCM microcapsules can be significantly reduced with this new microencapsulation method. In addition, thanks to its hard, inorganic shell, CenoPCM also enjoys many distinct mechanical, chemical, and thermal advantages over existing polymer encapsulated PCM: (1) cenospheres exhibits much better mechanical properties than the polymeric shells used in existing MEPCMs. The crushing strength of cenospheres are in the ranges from 10-20 MPa [20], which means cenospheres will not be easily damaged during handling and are able to withstand mechanical loading to some extent; (2) cenosphere shell has high thermal and chemical stability that can resist chemicals, lights, and high temperature; (3) since the shell of cenospheres are inorganic composed mainly of polycrystalline dense mullite, their thermal conductivity is much higher than the polymeric shells in existing MEPCMs. With all these advantages, encapsulating PCM with cenospheres is possible to eliminate the major barriers preventing the extensive application of MEPCMs in traditional building materials.

In this work, n-octadecane was selected as PCM to manufacture CenoPCM because of its good performance of heat energy storage and thermal regulation in an appropriate phase change range (23-28 °C) which is comfortable for the human body. The morphological-chemical performance and thermal energy storage properties of produced CenoPCM were characterized by XRF, SEM, TG, and DSC analysis techniques. A prototype thermally active cement mortar integrated with CenoPCM was also developed and evaluated for its physical, mechanical, and microstructural features. These analysis results showed the superior thermal and mechanical performance of the CenoPCM itself as well as mortar integrating CenoPCM.

2. Materials and methods

2.1. Materials

Reagent grade n-octadecane ($C_{18}H_{38}$), ammonium fluoride (NH_4F) with a purity of 96%, and 50% silicon dioxide in water (silica sol) were purchased from Alfa Aesar Company, USA. Hydrochloric acid (HCl) was commercially obtained from VWR International (USA). Calcium gluconate gel was always present during handling of hydrofluoric based acid solution (1.0 M NH_4F-1.2 M HCl-H_2O).

Cenospheres used in this research were obtained from CenoStar Corporation (USA). It has sizes between 10 and 200 µm with d_{10} = 59.4 µm, d_{50} = 96.7 µm and d_{90} = 137.2 µm, as shown in Fig. 1. Table 1 shows the chemical composition of cenospheres used, gained by X-ray fluorescence (XRF) analysis. According to the table, the cenospheres contain up to 57.35 wt% silicon dioxide, 31.93 wt% aluminum oxide, and lower amounts of iron, calcium, titanium, magnesium, sodium, potassium, and boron oxides, which range from less than one to three percent. The composition of Type I Portland cement used for casting mortar is also listed in Table 1, which was phased from Sakrete (USA).

2.2. *Three-step procedure to produce CenoPCM*

In this study, an innovative microencapsulation technology of PCM with cenospheres is developed to remove the technical barriers that prevent extensive applications of MEPCMs in construction materials. This new method consists of three steps: perforating cenospheres with acid etching, loading liquid PCM into perforated cenospheres, and sealing the PCM loaded cenospheres with silica sol.

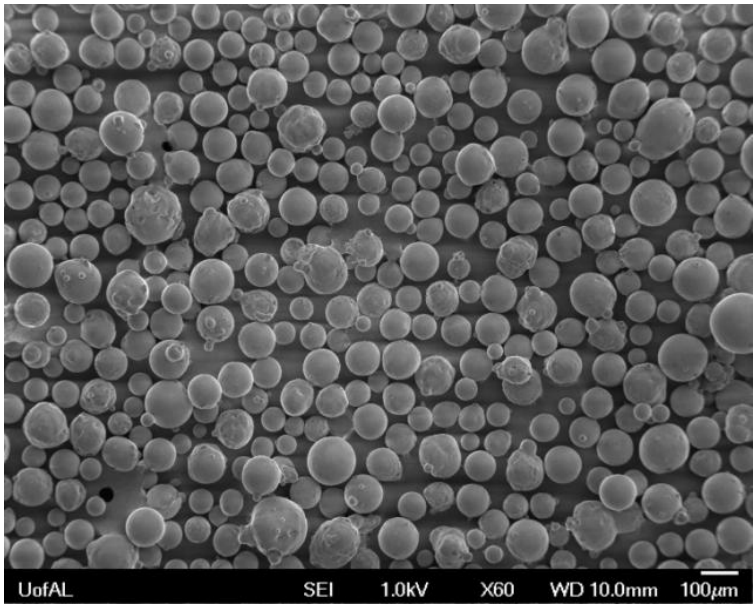

Fig. 1. As-received cenospheres with typical size from 10 to 200 μm.

Table 1 Chemical composition of cenospheres and Type I Portland cement.

Compound (%)	As-received Cenospheres	Type I Portland Cement
SiO_2	57.35	22.93
Al_2O_3	31.93	4.68
CaO	0.44	64.04
Fe_2O_3	2.27	2.41
TiO_2	1.17	0.20
MgO	0.54	3.38
Na_2O	0.54	0.23
K_2O	1.40	0.76
P_2O_5	0.06	0.08
MnO	N/A	0.07

2.2.1. Perforate cenospheres with acid etching

Cenosphere particle has an aluminosilicate shell with high stiffness and strength and a thickness in a few micrometer (Fig. 2(a)). The shell has a porous structure formed by gas inclusion and is covered by a glass-crystalline nanosize film, which is shown in Fig. 2 (b). The

141 hollow structure of cenospheres makes it an ideal material to encapsulate PCM. However, to
142 introduce PCM into cenospheres, the film covering the surface must be removed. This can be
143 done by acid etching the cenospheres [21,22]. To this end, approximately 12 g of cenospheres
144 was soaked into 250 mL of 1.0 M NH_4F-1.2 M HCl-H_2O solution for 2 hours with occasional
145 stirring. The specific gravity of cenospheres used is about 0.75 g/cm^3, thus 12 g of cenospheres
146 corresponded to a volume of 16 mL. This made the volume ratio of solid to liquid to 1:15 in this
147 acid treatment, which was among the range adopted by other researchers [21,22]. Occasional
148 stirring was applied instead of continuous one to prevent the possible damage of the cenospheres
149 during stirring. To compensate for this mild stirring process, longer treatment time was used (2
150 hours). By the end of this treatment, more than 95% of cenosphere sank to the bottom of
151 container (Fig. 3(b)), which was floating on the surface of acid solution at the beginning (Fig.
152 3(a)). The settlement of cenospheres indicates the completion of perforation. After etching, the
153 perforated cenospheres were vacuum filtered and rinsed with 1500 mL of water, followed by
154 dried in an oven at 150 °C. For this etching treatment, further work will be implemented on
155 optimizing the etching parameters in the future, including acid concentration, solid to liquid ratio,
156 and treatment time, among others.

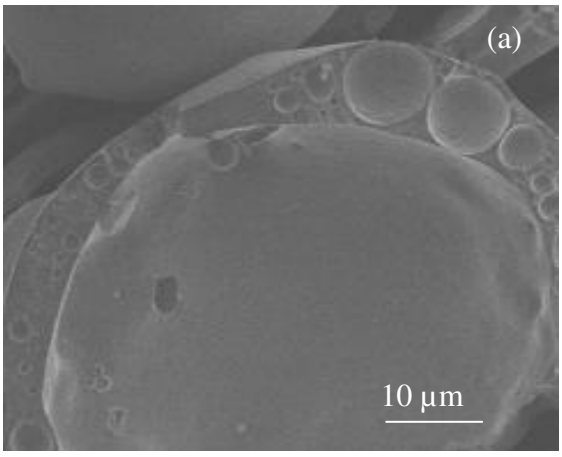

157

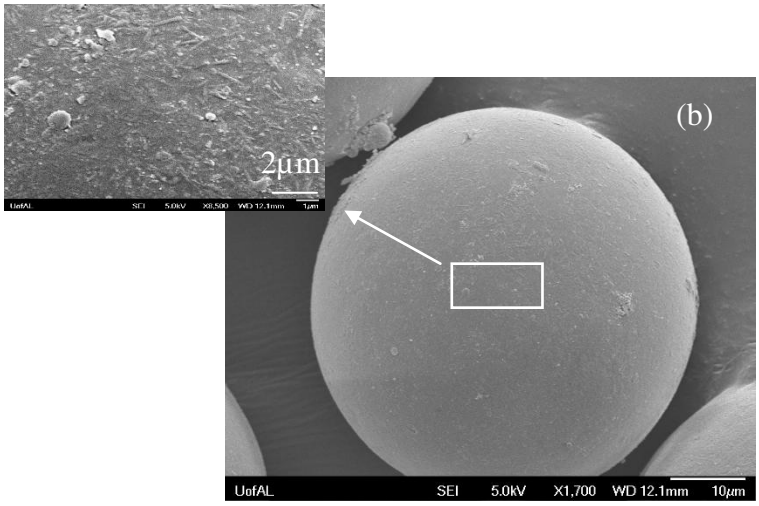

Fig. 2. Microstructure of cenospheres under SEM observation: (a) porous shell of cenospheres; and (b) impermeable shell before etching.

2.2.2. Load PCM into perforated cenospheres

Loading of PCM into perforated cenospheres was implemented via a vacuum impregnation process. The set up for the loading is shown as in Fig. 4. The dry perforated cenospheres was weighted and placed into a flask. The flask was exposed to vacuum pressure of approximately 80.5 kPa for ~ 2 hours [23]. Melted n-octadecane with volume as three times as the cenospheres was then introduced into the flask. Operation of the vacuum was stopped and air was allowed back into the flask to drive the n-octadecane into the hollow space inside the cenospheres for about 30 minutes. The completion of loading was achieved when the cenospheres settled down at the bottom of the flask. Before allowing the air back, all cenospheres were floating on the surface of liquid n-octadecane. During the whole impregnation process, the flask was heated by a hot plate with the temperature set at 60 ^{o}C. This temperature was high enough to keep the PCM in liquid status once it was introduced into the flask. This means the cenospheres were soaked in liquid PCM all the time when they contacted with each other. With completion of loading, flask

was quickly removed from the hot plate for cenospheres to be filtered and washed by 60 °C water. Then the cenospheres were left to be dried in air for about 48 hours.

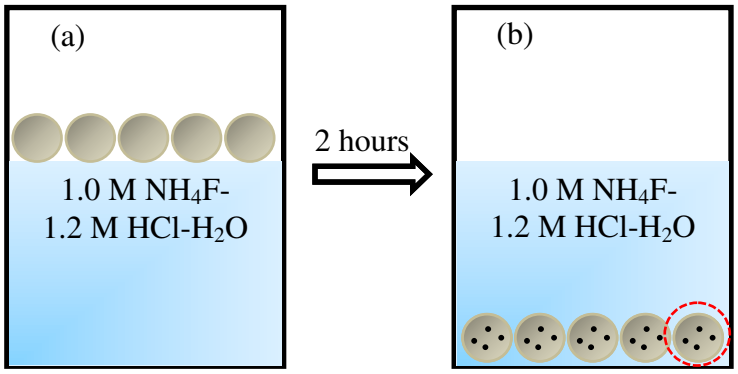

Fig. 3. Acid etching of cenospheres: (a) at the beginning, cenospheres floated on the surface of acid solution; (b) by the end of 2 hours' etching, cenospheres were perforated and sank to the bottom of the container.

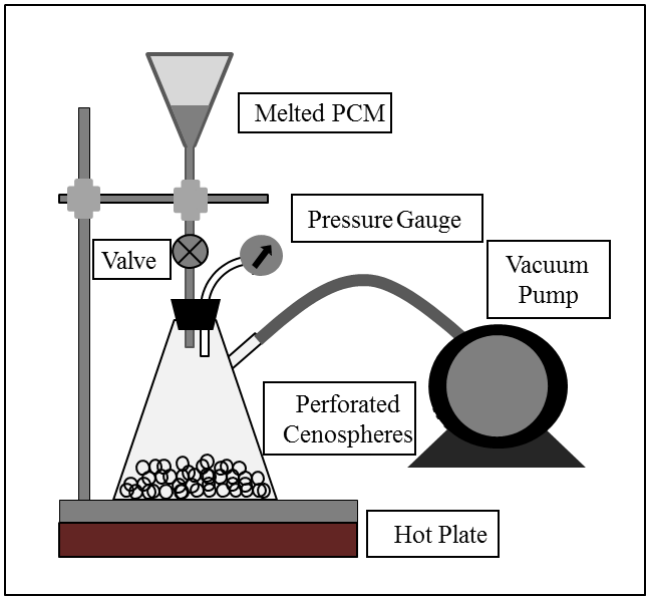

Fig. 4. Schematic drawing of vacuum loading setup.

2.2.3. Seal PCM loaded cenospheres with silica sol

To prevent the possible leakage of the loaded PCM, it is necessary to seal the pores created on the shell of perforated cenospheres. In this work, the pore sealing was done by coating a thin

192 layer of silica on the cenosphere shell. This coating will also strengthen the cenospheres.
193 Additionally, the coated silica layer would serve as a source of silica that can react with calcium
194 hydroxide formed from cement hydration [24,25]. The reaction will produce C-S-H gel, which is
195 the main bonding material that provides concrete strength. Thus, with the silica coating,
196 CenoPCM is possible to achieve a better bonding with the adjacent mortar materials when it is
197 integrated into mortar. The silica coating was simply done by soaking the PCM loaded
198 cenospheres into 25% silica sol for about 20 minutes at room temperature. The volume ratio
199 between cenospheres and silica sol was about 1:3, and during soaking the magnetic stirring with
200 a speed of 60 rpm was occasionally applied for more homogenous effect. Then the coated
201 cenospheres were filtered and dried over air. More work will be carried out in the future to find
202 the optimal coating parameters, including the content of cenospheres and silica sol, stirring speed,
203 and soaking, among others.

204 *2.3. Characterization of CenoPCM*

205 The morphology and microstructure of as-received cenospheres (see Figs. 1 and 2),
206 perforated cenospheres, PCM loaded cenospheres (unsealed CenoPCM), and sealed CenoPCM
207 were investigated using a JOEL 7000 FE scanning electron microscope (SEM). The microscope
208 was operated at low accelerating voltage (1~3 kV) and 10 mm working distance with a spot size
209 of medium 8. The phase change temperatures and enthalpies of the prepared CenoPCM were
210 determined using a DSC instrument (Q2000 from TA Instruments) at a scanning rate of 5°C/min
211 scanning rate. The scanning range was set at 10 to 50 °C. Thermogravimetric analysis (TGA)
212 was performed to examine the thermal stability of the produced CenoPCM by Q500 (from TA
213 instruments) at a heating rate of 20 °C/min between room temperature and 700 °C under nitrogen
214 atmosphere.

215

216 *2.4. Evaluation of mortar with CenoPCM*

217 Both sealed and unsealed CenoPCM was integrated into mortar to evaluate its effects on
218 mortar's physical, mechanical, and microstructural properties. The mix proportions are listed in
219 Table 2. There were three mix proportions used, the reference mortar without CenoPCM and the
220 mortars integrated with 3% PCM by total weight of the mortar through sealed or unsealed
221 CenoPCM. For all the mixes, the water to cement and sand to cement ratio are 0.55 and 3.0,
222 respectively. In the reference mortar without CenoPCM, fine sand that passed through No.30
223 sieve (~600μm) was added in the same volume as occupied by CenoPCM in 3% mortar. The
224 mean particle size of the fine sand was about 300 μm, estimated from the sieve analysis results.
225 With the known specific gravity of the materials used (3.15 for cement, 2.7 for sand, 0.75 for
226 cenospheres) and loading capacity of cenospheres with PCM (175.02 wt.% obtained from TGA),
227 the needed amount of each material can be easily calculated, and the results are shown in Table 2.
228 It has to be pointed out that no superplasticizer was used in the mix proportions. This is because
229 the mixes already showed similar flowability and workability during mixing and casting without
230 superplasticizers. Thus the adjustment of superplasticizer was not required in this study.

231 **Table 2** Mix proportions of mortars.

Constituent	Reference Mortar		3% Mortar	
	Volume (m^3)	Mass (kg)	Volume (m^3)	Mass (kg)
Cement	0.15	480	0.15	480
Water	0.26	264	0.26	264
Sand	0.53	1440	0.53	1440
Fine Sand	0.05	135	0	0
Unsealed or Sealed CenoPCM	0	0	0.05	106
Total % PCM in Mortar	0	0	5	3

232 Cement, water, and sand were firstly mixed together according to the ASTM C305 [26].
233 Then CenoPCM or fine sand was introduced to the mixture and mixed for additional 2 minutes at
234 slow speed to produce homogenous mortar. Thereafter, the mortar was cast into cylindrical
235 molds with a diameter of 50mm and height of 100 mm, and then compacted using a vibration
236 table. After being seal cured for 24 hours, the samples were demolded and cured under water at a
237 controlled temperature of 23±1°C till the designated ages of 3, 7, and 28 days. At each age,
238 compression test was carried out on three samples according to the ASTM C109 [27]. The
239 mortar samples were prized into pieces for SEM observation as well.

240 **3. Results and discussion**

241 3.1 Microstructure of perforated cenospheres, unsealed CenoPCM, and sealed CenoPCM

242 The original cenospheres represent a silicate-alumina-iron multiple component system with
243 the surface covered by glass-crystalline nanosize film. To use cenospheres for
244 microencapsulation, this layer of film should be removed to make the inner hollow space
245 accessible for PCM. In current work, this was achieved by etching the cenospheres with a
246 solution of 1.0 M NH_4F-1.2 M HCl-H_2O for 2 hours. Table 3 lists the chemical composition of
247 cenospheres after this acid treatment. Compared to the original composition (Table 1), the
248 content of alumina was increased significantly from 31.93 to 35.00% in the perforated
249 cenospheres. This is because alumina was not subjected to the etching action [21], while the
250 silica and iron deposits on cenospheres were dissolved by the hydrofluoric based acid system.
251 The dissolution resulted in about 8.77% weight loss of the cenospheres shell. This small amount
252 of dissolution indicates that the acid etching is able to perforate the shell without compromising
253 the shell's mechanical strength.

Fig. 5 shows the microstructure of the perforated cenospheres. It can be seen clearly that compared to the original cenospheres (Fig. 2(b)), the wall structure changes significantly, going from a solid to a spongy porous one. This indicates that the glass-crystalline film has been removed from the cenosphere surface by the applied acid treatment. From Fig. 5, it is also seen that the majority of pores created on cenosphere shell are smaller than 500 nm, with occasional pores with micron size (< 2μm). These pores, together with the porous structure of cenosphere shell formed by gaseous inclusions, perforated the cenospheres, providing paths for loading liquid PCM.

Table 3 Chemical composition of perforated cenospheres produced by acid etching.

Compound (%)	Perforated Cenospheres
SiO_2	57.81
Al_2O_3	35.00
CaO	0.33
Fe_2O_3	2.13
TiO_2	1.15
MgO	0.51
Na_2O	0.52
K_2O	1.32
P_2O_5	0.05

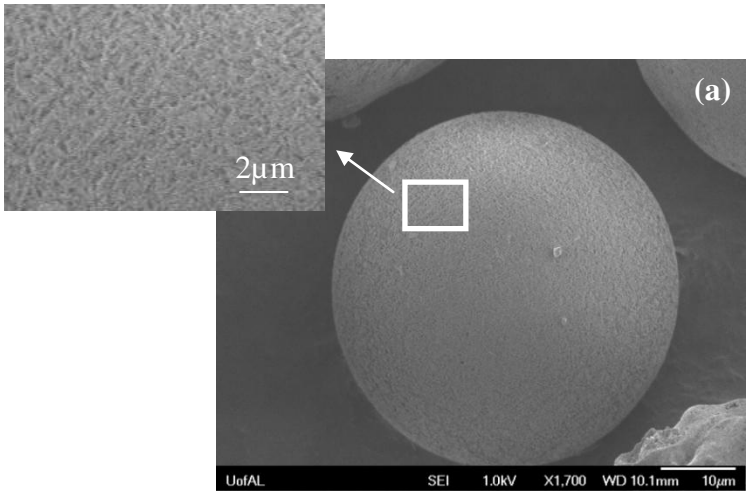

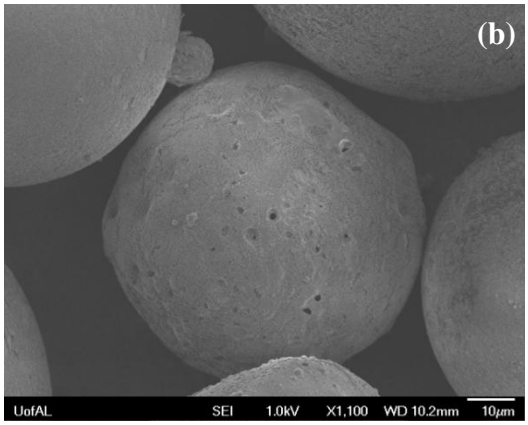

Fig. 5. SEM microphotographs of the perforated cenospheres after being etched with 1.0 M NH_4F-1.2 M HCl-H_2O solution for 2 hours.

The micrographs of cenospheres with loaded PCM via the vacuum impregnation process are demonstrated in Fig. 6. From Fig. 6(a), it can be found that almost all the PCM loaded cenospheres are intact. This means that the vacuum pressure applied (80.5 kPa) for PCM impregnation did not destroy the shells, suggesting both the applicability of vacuum loading and high mechanical strength of perforated cenospheres. To expose the internal space of cenospheres, the spheres were carefully crushed by a small piece of slug. Examination of these purposely broken cenospheres (Fig. 6(b)) suggests that they all are filled with PCM. For clarity, the ones in the upper right corner and center of Fig. 6(b) are enlarged and displayed in Figs. 6(c) and (d), respectively. It is interesting to see from these two figures, especially Fig. 6(d), that the detached pieces have not yet completely fell down from their original positions in the cenospheres. This indicates that the particle is damaged during the manual broken process right before SEM observation, instead of being originally broken before or during impregnation. Otherwise, these pieces would fully fall apart into surroundings. From the gaps between these broken pieces, it can be seen that the cenospheres are fully loaded with PCM that has a layered structure.

The last step involved in preparing CenoPCM was to seal the perforated cenospheres to prevent the possible leakage of PCM during its service life. This coating was applied by simply soaking the PCM loaded cenospheres into silica sol. Fig. 7 shows the cenospheres being coated with silica sol. Fig. 7(b) displays the same cenosphere particle in the center of Fig. 7(a) but at a higher magnification. According to Fig. 7(b), the surface texture of the cenosphere has been coarsened with coating, compared to the ones without coating (Figs. 5 and 6). The silica particles from the sol connect with each other, forming a layer of coating covering the cenosphere shell. One may also notice that a few pores with sizes of about 2 μm are still visible on the shell after cenosphere being coated, which indicates that the coating layer is thin and not thick to the extent that can cover the micron size pores. Increased thickness of the coating will be facilitated in the future research by optimizing the coating parameters, including the content of cenospheres and silica sol, stirring speed, and soaking time, among others.

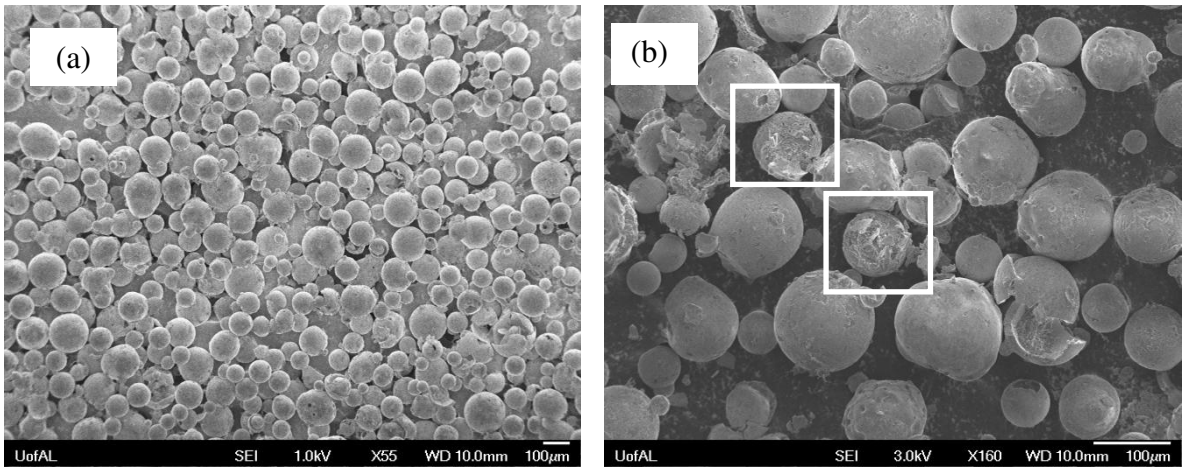

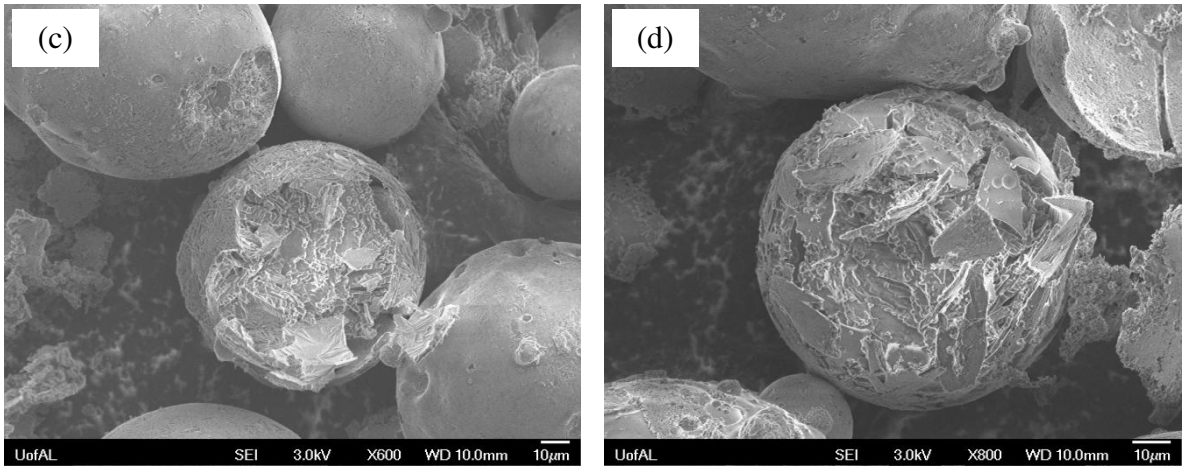

Fig. 6. (a) Microstructure of cenospheres loaded with PCM before manual crushing; (b), (c), and (d) manually crushed cenospheres whose internal space is fully loaded with PCM.

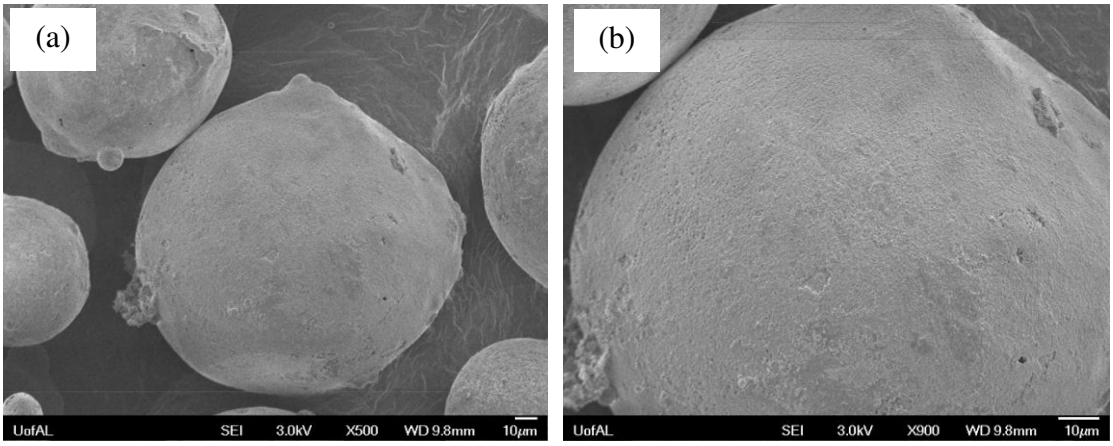

Fig. 7. Coating of a silica layer on the surface of perforated cenospheres loaded with PCM.

3.2. Thermal stability and phase-change performance of CenoPCM

Thermal stability is a significant factor in evaluating CenoPCM for the application of heat energy storage and thermal regulation. The thermal stability of unsealed CenoPCM was investigated by means of TGA, which presents the mass loss of samples and corresponding temperature. The TGA curve is depicted in Fig. 8. A sharp weight loss starts at around 130 °C, which was attributed to the decomposition of the microencapsulated PCM (n-octadecane) [28]. Decomposed PCM vapor was quickly lost from the perforated cenospheres, and this process

continued till temperature reached 220 °C. After this temperature, no further weight loss can be observed for the CenoPCM sample, suggesting that all n-octadecane inside the perforated cenospheres had been evaporated. The residual weight of the sample is the weight of the perforated cenosphere shell. The curve shows that the loaded PCM accounts for approximately 63.64% by total weight of the produced CenoPCM, which corresponds to as high as 175.02% loading capacity of perforated cenospheres with n-octadecane. From the curve, it is also seen that there is no degradation occurring in the cenosphere shell within the testing temperature range (700 °C), implying the much higher thermal stability of the cenosphere than polymer shells used in existing MEPCMs. The polymer based microcapsules would have another obvious weight loss at the decomposition temperature of the shell materials [28].

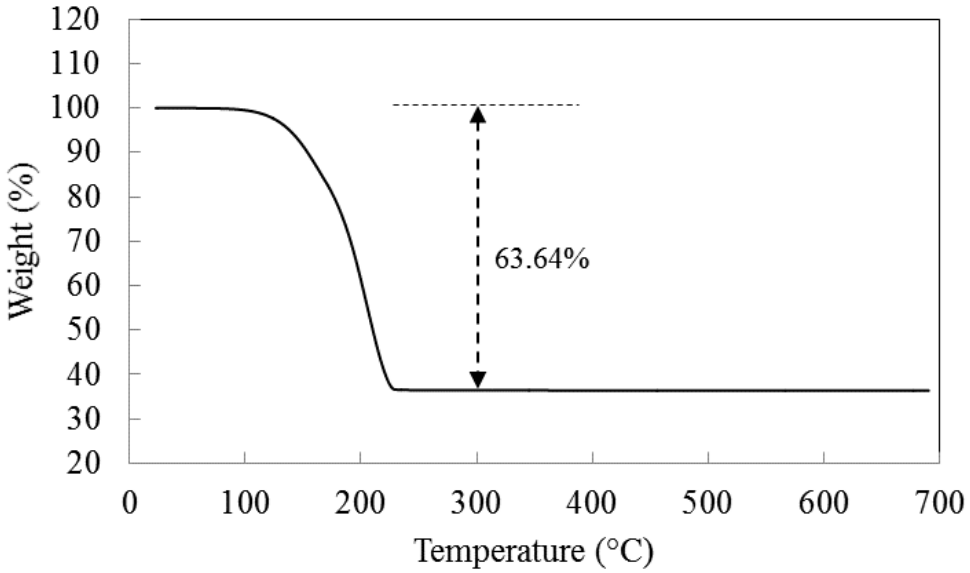

Fig. 8. TGA thermogram of the produced CenoPCM.

The phase change behaviors of the prepared CenoPCM (unsealed) are evaluated by DSC, and its thermograph is presented in Fig. 9, where the upward peak indicates the exothermic process while the downward corresponds to the endothermic one. The phase change temperatures (i.e. T_m

and T_c) of the CenoPCM obtained from the DSC measurement are also displayed in the figure. T_m or T_c is given by the intersection of the tangent through the point of maximum slope on the melting or crystallization front peak and the extrapolated baseline on the DSC heating and cooling curves, respectively. The produced CenoPCM has a crystallization peak T_c at around 22.7°C, and it is as well observed that the peak is not that sharp. This is because n-octadecane has two types of structures that crystallize at slightly different temperatures, generating two exothermic peaks that are overlapped together [28]. On the contrary, the n-octadecane shows only one single, well-defined endothermic peak on the heating thermogram with T_m at 23.8 °C. The phase-change enthalpies [i.e., the fusion heat (ΔH_m) and crystallization enthalpy (ΔH_c)] of the CenoPCM are deduced from the DSC measurement and also shown in Fig. 9. The CenoPCM has a ΔH_m of 119.83 J/g and ΔH_c of 128.84 J/g, respectively.

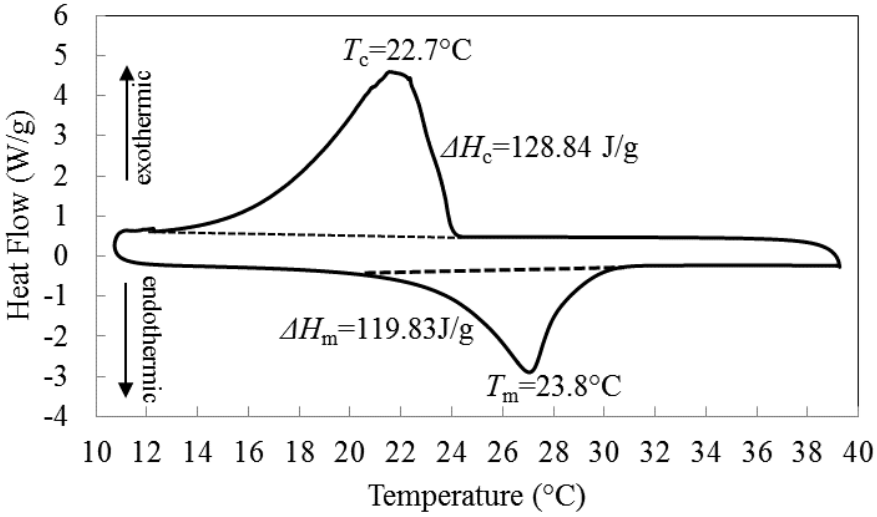

Fig. 9. DSC thermograms of the produced CenoPCM.

3.3. Mechanical property of cement mortar incorporating CenoPCM

To examine the mechanical performance of CenoPCM in construction materials, the compressive strength of mortar with and without CenoPCM is measured and displayed in Fig. 10. From this figure, it can be seen that compared to the control mortar, addition of 3.0 wt.% of PCM

through either unsealed or sealed CenoPCM (corresponding to ~4.7 wt.% of CenoPCM) resulted in the strength loss at all the ages studied, which was around 15.6% and 5.6% at 28 days, respectively. But both mortars remain strong enough for structural application. The lowest strength in the mortar containing unsealed CenoPCM could be partially attributed to the PCM absorbed on the shell surface. The PCM may interact or crosslink with unreacted cement constituents and hydration products, which potentially reduces the strength [11,12]. After the CenoPCM being coated with a layer of silica sol, the strength has been recovered, which reached 94.4% of the control mortar at 28 days. This could be caused by the fact that the silica sol seals the perforated pores on the shell, densifying and strengthening the CenoPCM particles. In the meantime, the coated silica sol may react with calcium hydroxide, producing C-S-H gel that can enhance the bonding between the CenoPCM microcapsules and surrounding mortar microstructure. As comparison, after adding 3wt.% of CIBA's and BASF's phase change materials microcapsules, the strength reduction of mortar was about 44% [11] and 47% [12] at 28 days, respectively. This is because the polymer encapsulated PCMs do not present a mechanical resistance, their inclusions into concrete weaken the overall strength of the materials [11,12]. On the contrary, the much lower strength reduction in CenoPCM mortars should be attributed to the high mechanical strength properties of the cenospheres shell. As given by the manufacturer, 90% of the cenospheres used in current work can resist compression up to 22.06 MPa.

The microstructure of mortar with unsealed CenoPCM was investigated. The samples were prepared as small fragment from the failed cylindrical mortar specimens after compression tests. The fragments were mounted on Al stubs with carbon cement, vacuum dried for 24 hours, Pt sputter coated, and imaged in the high vacuum SEM mode. Evidence of CenoPCM particles was

found to be well distributed throughout the hardened microstructure, and it was apparent in the form of intact CenoPCM particles (labelled as "A" in Fig. 11), hemispherical voids (characteristic of CenoPCM particle shape and surface texture) from where CenoPCM particles were present during curing then later pulled out because of compression (labelled as "B" in Fig. 11), or damaged CenoPCM particles still occupying the voids (labelled as "C" in Fig. 11).

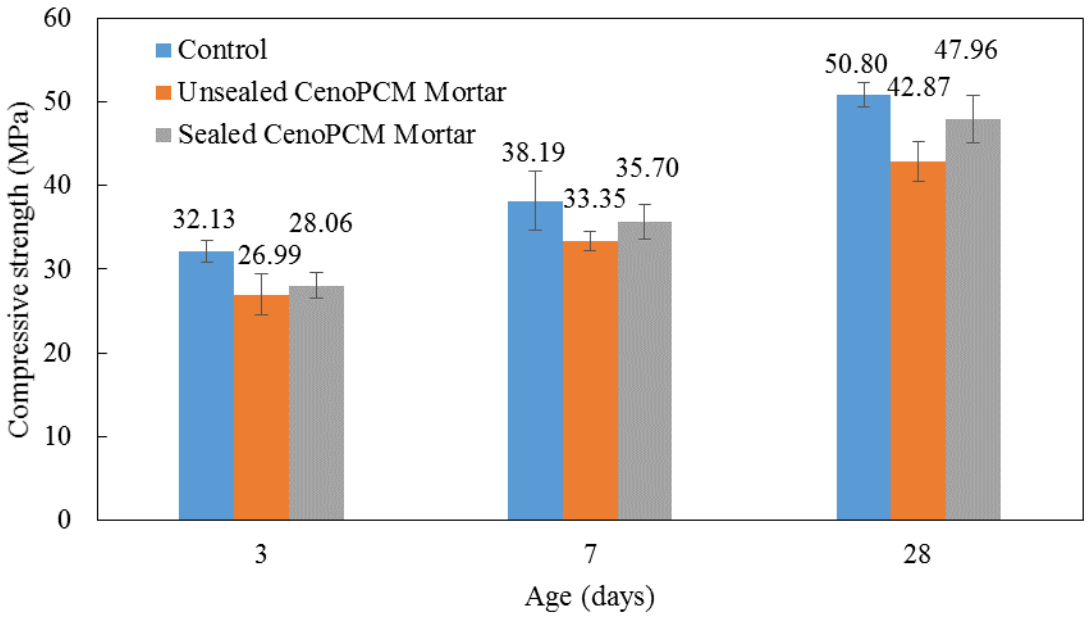

Fig. 10. Compressive strength of mortars with and without CenoPCM at different ages.

Close-ups of typical B and C spots shown in Fig. 11 are shown in Fig. 12 (a) and (b), respectively, to illustrate the difference of these two microstructures. From these two images, it is clear to see that the spherical voids (Fig. 12 (a)) do not have the characteristic porous wall as seen in the damaged cenospheres. But the voids have the typical cenospheres' spherical shape and surface texture, so they were not air void induced during mortar mixing. Instead, they appeared to be created by the bursting of cenospheres, which were the result of CenoPCM particle pre-curing embedment followed by post-loading pull-out. The damaged CenoPCM remnants (Fig. 12 (b)) are not because that the CenoPCM were damaged during mortar mixing or

compaction, but they are merely a consequence of the compression cutting its way through the capsules because of their weaker strength when compared to the surrounding matrix. If CenoPCM was broken during mortar mixing or compaction, at least some of the damaged CenoPCM particles would be filled with mortar instead of being hollow. But there is little evidence found for such broken particles. The survival of CenoPCM particles during mortar manufacturing should be attributed to the high crushing strength of cenospheres (10-20MPa). Compared to those MEPCMs which were easily damaged [12], CenoPCM is more applicable to be used in concrete materials for thermal energy storage given to its superior mechanical performance.

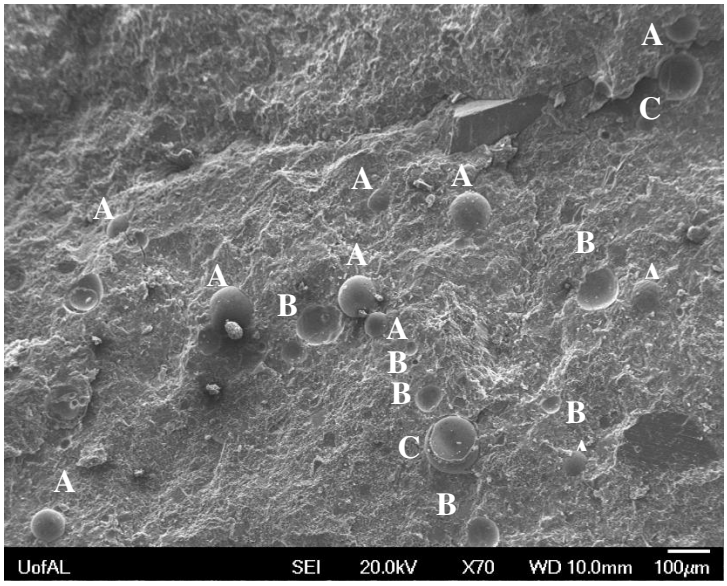

Fig. 11. SEM micrograph of CenoPCM (unsealed) mortar fracture surface showing (A) intact CenoPCM particles, (B) hemispherical voids from where CenoPCM particles were present during curing then later pulled out because of compression, and (C) damaged, hollow CenoPCM particles.

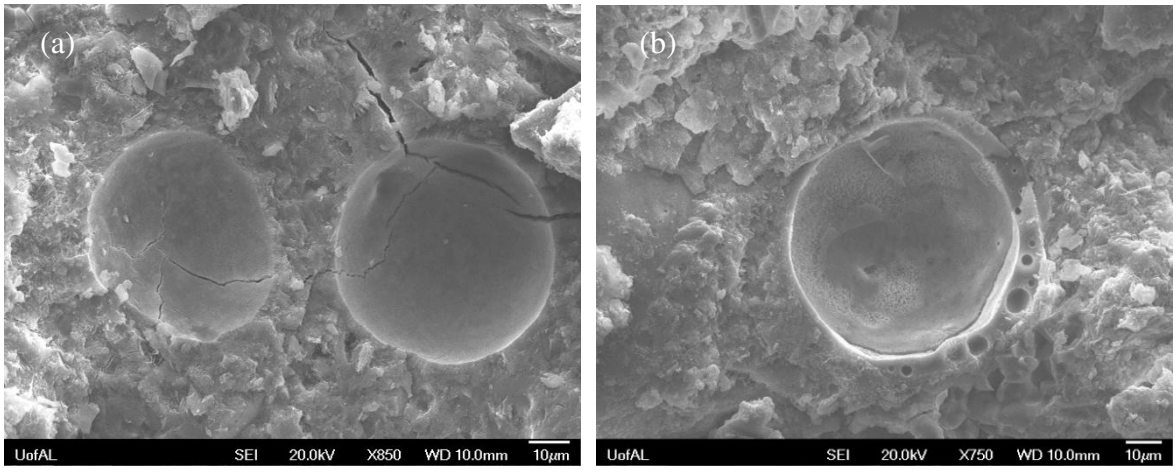

Fig. 12. (a) SEM images showing hemispherical voids due to cenosphere pulled out; (b) A damaged CenoPCM particle (unsealed) in the mortar at the hydration age of 28 days.

4. Conclusions

A novel technology to encapsulate PCM into cenospheres has been successfully demonstrated in this paper. By removing the nanosize glassy-crystalline film covering the cenosphere shell using chemical etching, perforated cenospheres can be produced. PCM in liquid phase can be easily loaded into the perforated cenospheres to produce PCM microcapsules (CenoPCM), which not only can store and release heat at the human comfort zone (T_c=21.57 °C and T_m=23.8°C), but also possesses high thermal storage and release capacities. Integration of 4.7% unsealed CenoPCM (corresponding to 3.0% pure PCM inclusion) into mortar caused 10-15% loss of compressive strength. However, such reduction in strength of mortar can be recovered by coating the CenoPCM with a thin layer of silica sol on the surface.

The new microencapsulation method developed in this study of PCM using cenospheres enjoys many advantages over currently available polymer-based MEPCMs, including low cost, high thermal energy storage capacity and stability, and high mechanical properties. This study also suggests that CenoPCM can be a promising candidate for adding thermal energy storage to

traditional construction materials such as concrete. More work will be carried out to evaluate the thermal performance, durability, and inflammability of concrete or mortar incorporating CenoPCM.

Acknowledgements

The financial supports from the National Science Foundation - United States (CMMI-1000580, 1563551) and the Research Stimulation Program, The University of Alabama are highly appreciated.

References

[1] WBCSD, (n.d.). http://www.wbcsd.org/publications-and-tools.aspx (accessed February 17, 2017).

[2] T. Khadiran, M.Z. Hussein, Z. Zainal, R. Rusli, Encapsulation techniques for organic phase change materials as thermal energy storage medium: A review, Sol. Energy Mater. Sol. Cells. 143 (2015) 78–98.

[3] Y. Zhang, G. Zhou, K. Lin, Q. Zhang, H. Di, Application of latent heat thermal energy storage in buildings: State-of-the-art and outlook, Build. Environ. 42 (2007) 2197–2209.

[4] N. Zhu, Z. Ma, S. Wang, Dynamic characteristics and energy performance of buildings using phase change materials: A review, Energy Convers. Manag. 50 (2009) 3169–3181.

[5] W. a. Qureshi, N.-K.C. Nair, M.M. Farid, Impact of energy storage in buildings on electricity demand side management, Energy Convers. Manag. 52 (2011) 2110–2120.

[6] A. Waqas, Z. Ud Din, Phase change material (PCM) storage for free cooling of buildings -

A review, Renew. Sustain. Energy Rev. 18 (2013) 607–625.

[7] P.C. Tabares-Velasco, C. Christensen, M. Bianchi, C. Booten, Verification and Validation of EnergyPlus Conduction Finite Difference and Phase Change Material Models for Opaque Wall Assemblies, Golden, Colorado, 2012.

[8] K. Biswas, J. Lu, P. Soroushian, S. Shrestha, Combined experimental and numerical evaluation of a prototype nano-PCM enhanced wallboard, Appl. Energy. 131 (2014) 517–529.

[9] V. V. Tyagi, S.C. Kaushik, S.K. Tyagi, T. Akiyama, Development of phase change materials based microencapsulated technology for buildings: A review, Renew. Sustain. Energy Rev. 15 (2011) 1373–1391.

[10] R. Russell, S.S. Sunder, P. D. Domich, "Federal Research and Development Agenda for Net-Zero Energy , High-Performance Green Buildings." Report of the Subcommittee on Buildings Technology Research and Development, 2008.

[11] J. Giro-Paloma, M. Mart??nez, L.F. Cabeza, A.I. Fern??ndez, Types, methods, techniques, and applications for microencapsulated phase change materials (MPCM): A review, Renew. Sustain. Energy Rev. 53 (2016) 1059–1075.

[12] M. Hunger, A.G. Entrop, I. Mandilaras, H.J.H. Brouwers, M. Founti, The behavior of self-compacting concrete containing micro-encapsulated Phase Change Materials, Cem. Concr. Compos. 31 (2009) 731–743.

[13] L. Zhao, H. Wang, J. Luo, Y. Liu, G. Song, G. Tang, Fabrication and properties of microencapsulated n-octadecane with TiO2 shell as thermal energy storage materials, Sol.

Energy. 127 (2016) 28–35.

[14] B. Li, T. Liu, L. Hu, Y. Wang, L. Gao, Fabrication and Properties of Microencapsulated Paraffin@SiO 2 Phase Change Composite for Thermal Energy Storage, ACS Sustain. Chem. Eng. 1 (2013) 374–380.

[15] B. Xu, Z. Li, Paraffin/diatomite composite phase change material incorporated cement-based composite for thermal energy storage, Appl. Energy. 105 (2013) 229–237.

[16] B. Xu, Z. Li, Performance of novel thermal energy storage engineered cementitious composites incorporating a paraffin/diatomite composite phase change material, Appl. Energy. 121 (2014) 114–122.

[17] B. Xu, H. Ma, Z. Lu, Z. Li, Paraffin/expanded vermiculite composite phase change material as aggregate for developing lightweight thermal energy storage cement-based composites, Appl. Energy. 160 (2015) 358–367.

[18] M. Kheradmand, J. Castro-Gomes, M. Azenha, P.D. Silva, J.L.B. De Aguiar, S.E. Zoorob, Assessing the feasibility of impregnating phase change materials in lightweight aggregate for development of thermal energy storage systems, Constr. Build. Mater. 89 (2015) 48–59.

[19] M. V Pankova, E. V Fomenko, N.N. Anshits, T.A. Vereshchagina, A.G. Anshits, Microspherical Carriers and Adsorbents for the Processes in Corrosive Media, Chem. Sustain. Dev. 18 (2010) 509–516.

[20] P.P. Bartake, D.N. Singh, Determination of Crushing Strength of Cenospheres, J. ASTM Int. 2 (2005) Paper ID JAI13092.

[21] E. V. Fomenko, A.A. Bobko, A.N. Salanov, I.A. Kirilyuk, I.A. Grigor'ev, V. V. Khramtsov, et al., Perforated cenosphere supported pH sensitive spin probes, Russ. Chem. Bull. 57 (2008) 493–498.

[22] Y. Xie, S.D. McAllister, D.B. Edwards, I.F. Cheng, Fabrication of porous hollow glass microspheres, J. Power Sources. 196 (2011) 10727–10730.

[23] L. Liston, M. Krafcik, Y. Farnam, B. Tao, K. Erk, J. Weiss., Toward the use of phase change materials (PCM) in concrete pavements: Evaluation of thermal properties of PCM., in: 2014 FAA Worldw. Airpt. Technol. Transf. Conf. Innov. Airpt. Saf. Pavement Technol., Galloway, NJ, 2014: pp. 1–13.

[24] D.J. Corr, S.P. Shah, Final report:design and application of high-volume fly ash self-consolidating concrete with the incorporation of nanoparticles, 2012.

[25] J.F. Muñoz, R.C. Meininger, J. Youtcheff, New Possibilities and Future Pathways of Nanoporous Thin Film Technology to Improve Concrete Performance, Transp. Res. Rec. J. Transp. Res. Board. 2142 (2010) 34–41.

[26] ASTM, C305-14: Standard Practice for Mechanical Mixing of Hydraulic Cement Pastes and Mortars of Plastic Consistency, West Conshohocken, PA, 2014.

[27] ASTM, C109/C109M-13: Standard Test Method for Compressive Strength of Hydraulic Cement Mortars (Using 2-in . or [50-mm] Cube Specimens), West Conshohocken, PA, 2010.

[28] H. Zhang, X. Wang, Synthesis and properties of microencapsulated n-octadecane with polyurea shells containing different soft segments for heat energy storage and thermal

496 regulation, Sol. Energy Mater. Sol. Cells. 93 (2009) 1366–1376.

497